

## Supplementary Data

*For*

### New Ce-doped MgAl-LDH@Au Nanocatalyst for Highly Efficient Reductive Degradation of Organic Contaminants

*Kanwal Iqbal,<sup>a</sup> Anam Iqbal,<sup>a</sup> Alexander M. Kirillov,<sup>b</sup> Bingkai Wang,<sup>a</sup> Weisheng Liu,<sup>a</sup> Yu Tang<sup>\*a</sup>*

<sup>a</sup> State Key Laboratory of Applied Organic Chemistry, Key Laboratory of Nonferrous Metal Chemistry and Resources Utilization of Gansu Province, College of Chemistry and Chemical Engineering, Lanzhou University, Lanzhou 730000, P.R. China

<sup>b</sup> Centro de Quimica Estrutural, Complexo I, Instituto Superior Técnico, Universidade de Lisboa, Av. Rovisco Pais, Lisbon 1049-001, Portugal

## Contents

**Fig. S1** FTIR spectra of MgAl-LDH, MgAlCe-LDH, MgAl-LDH@Au, and MgAlCe-LDH@Au.

**Fig. S2** SEM images of (a) MgAlCe-LDH, (b) MgAl-LDH@Au, and (c) MgAlCe-LDH@Au.

**Fig. S3** EDX spectrum of MgAlCe-LDH@Au.

**Fig. S4** High-resolution XPS spectra of MgAlCe-LDH@Au.

**Fig. S5** TGA curves of MgAl-LDH@Au and MgAlCe-LDH@Au.

**Fig. S6** Time-dependent UV-vis spectra of the reaction mixtures containing aqueous solutions of different dyes in the presence of NaBH<sub>4</sub> as a reducing agent and in the absence of catalyst (blank tests).

**Fig. S7** Time-dependent UV-vis spectra of the reaction mixtures containing aqueous solutions of different dyes in the presence of NaBH<sub>4</sub> as a reducing agent and MgAlCe-LDH@Au as a catalyst.

**Fig. S8** Calibration curves as a function of  $\ln(C_t/C_0)$  vs. reaction time for the reaction mixtures containing aqueous solutions of different dyes in the presence of NaBH<sub>4</sub> as a reducing agent and MgAlCe-LDH@Au as a catalyst.

**Fig. S9** Time-dependent UV-vis spectra of the reaction mixtures containing aqueous solutions of 4-NP or different dyes in the presence of NaBH<sub>4</sub> as a reducing agent and MgAl-LDH@Au as a catalyst.

**Fig. S10** Calibration curves as a function of  $\ln(C_t/C_0)$  vs. reaction time for the reaction mixtures containing aqueous solutions of 4-NP or different dyes in the presence of NaBH<sub>4</sub> as a reducing agent and MgAl-LDH@Au as a catalyst.

**Fig. S11** Time-dependent UV-vis spectra of the reaction mixtures containing aqueous solutions of 4-NP or different dyes in the presence of NaBH<sub>4</sub> as a reducing agent and MgAlCe-LDH as a catalyst.

**Fig. S12** Calibration curves as a function of  $\ln(C_t/C_0)$  vs. reaction time for the reaction mixtures containing aqueous solutions of 4-NP or different dyes in the presence of NaBH<sub>4</sub> as a reducing agent and MgAlCe-LDH as a catalyst.

**Table S1** Comparison of various catalytic systems for the reductive degradation of 4-NP.

**Table S2** Comparison of various catalytic systems for the reductive degradation of different dyes.

## Supplementary References

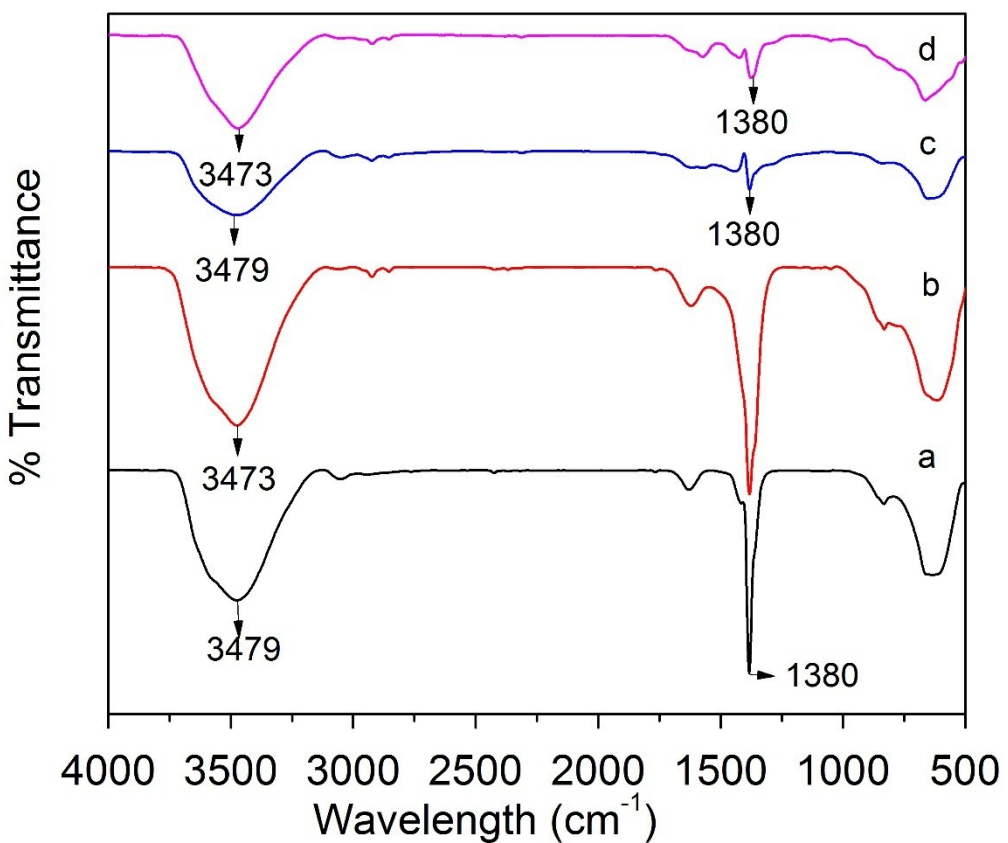


**Fig. S1** FT-IR spectra of MgAl-LDH (a), MgAlCe-LDH (b), MgAl-LDH@Au (c), and MgAlCe-LDH@Au (d)

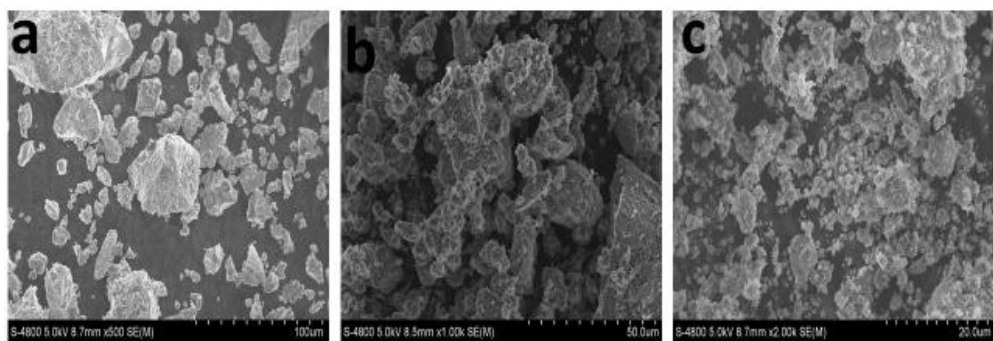


**Fig. S2** SEM images of (a) MgAlCe-LDH, (b) MgAl-LDH@Au, and (c) MgAlCe-LDH@Au.

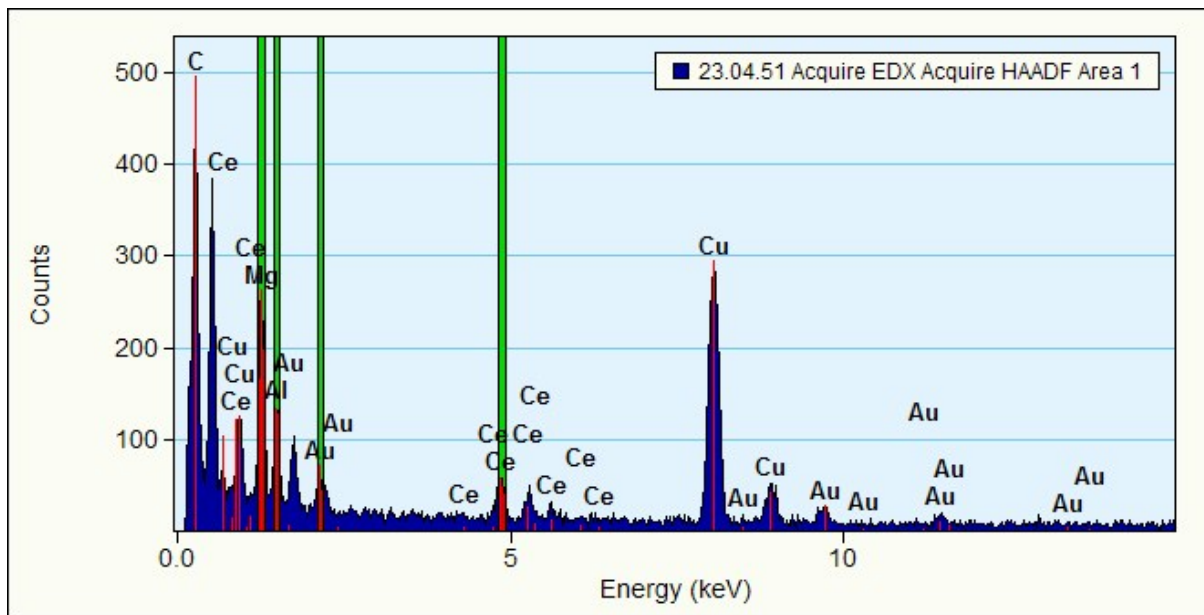


**Fig. S3** EDX spectrum of MgAlCe-LDH@Au. The Cu signals originate from Cu grid.

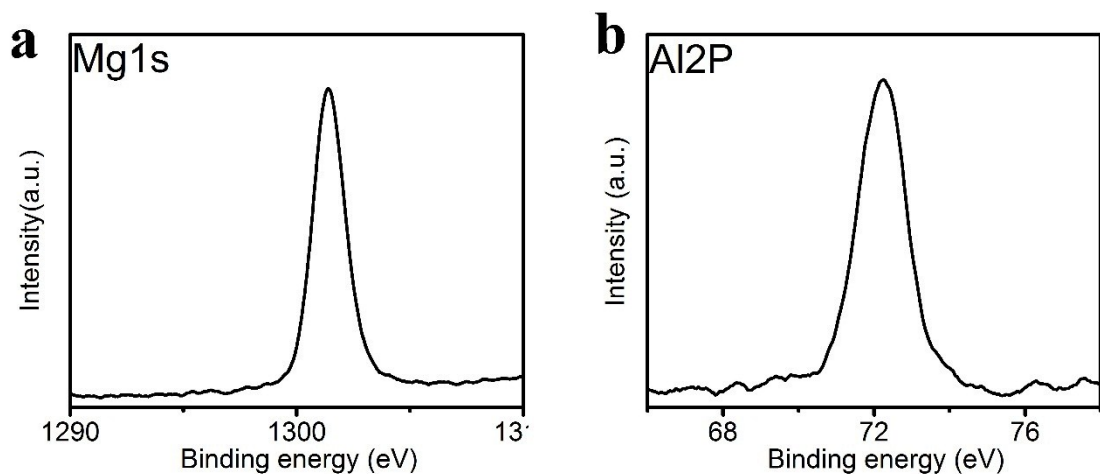


**Fig. S4** High-resolution XPS spectra of MgAlCe-LDH@Au: (a) Mg 1s, (b) Al 2p.

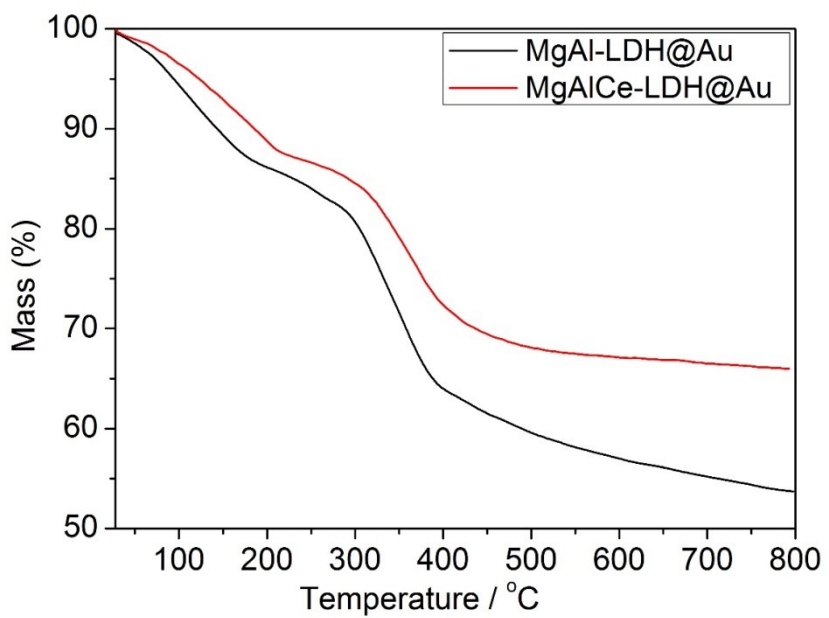


**Fig. S5** TGA curves of MgAl-LDH@Au and MgAlCe-LDH@Au.

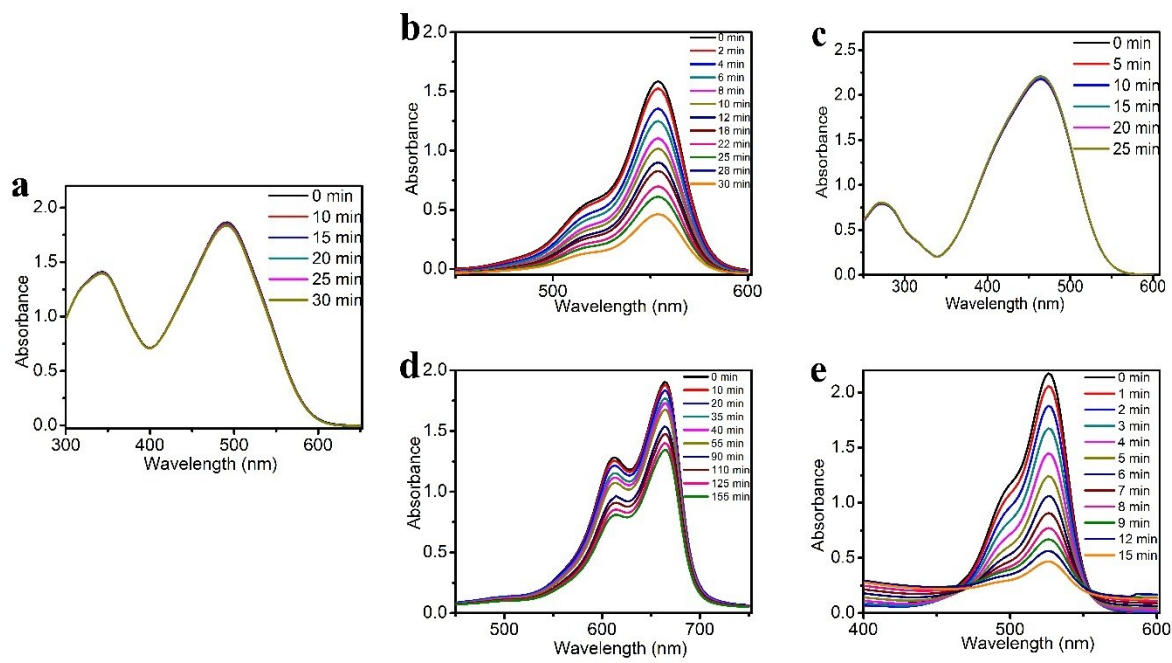


**Fig. S6** Time-dependent UV-vis spectra of the reaction mixtures containing (a) CR, (b) RhB, (c) MO, (d) MB, and (e) R6G aqueous solutions in the presence of  $\text{NaBH}_4$  as a reducing agent and in the absence of catalyst (blank tests). Reaction conditions: 2.5 mL aqueous solutions of (a) CR ( $6 \times 10^{-5}$  M), (b) RhB ( $2 \times 10^{-6}$  M), (c) MO ( $1 \times 10^{-4}$  M), (d) MB ( $3 \times 10^{-5}$  M), (e) R6G ( $4 \times 10^{-4}$  M ), and  $\text{NaBH}_4$  (0.1 M, 480  $\mu\text{L}$ ).

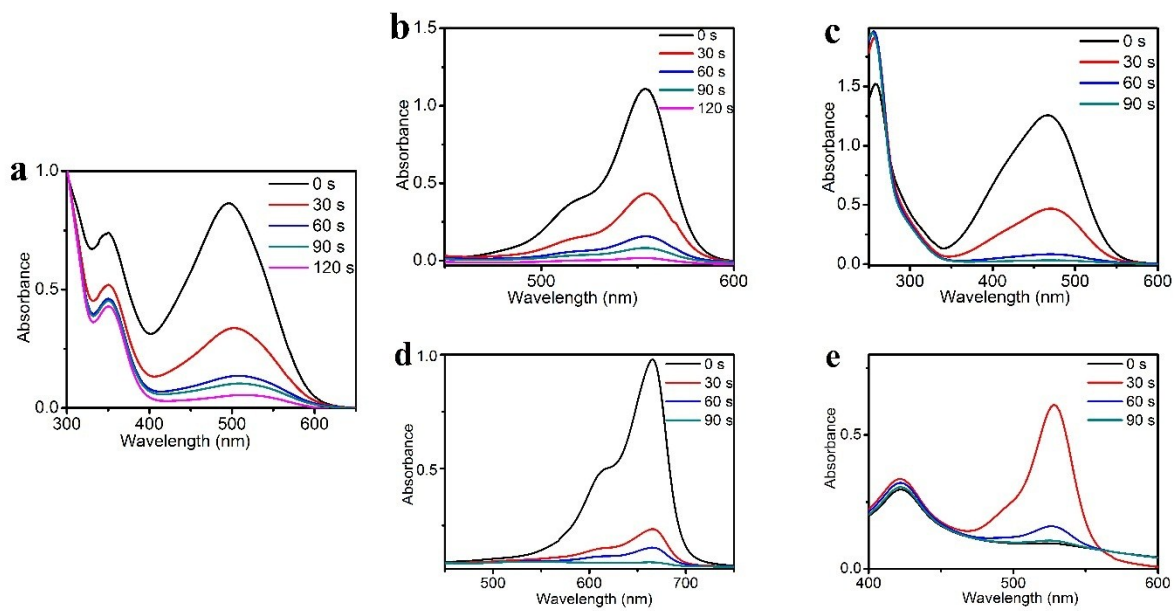


**Fig. S7** Time-dependent UV-vis spectra of the reaction mixtures containing (a) CR, (b) RhB, (c) MO, (d) MB, and (e) R6G aqueous solutions in the presence of  $\text{NaBH}_4$  as a reducing agent and  $\text{MgAlCe-LDH@Au}$  as a catalyst. Reaction conditions:  $\text{MgAlCe-LDH@Au}$  ( $20 \mu\text{L}$ ,  $1 \text{ mg/mL}$ ),  $2.5 \text{ mL}$  aqueous solutions of (a) CR ( $6 \times 10^{-5} \text{ M}$ ), (b) RhB ( $2 \times 10^{-6} \text{ M}$ ), (c) MO ( $1 \times 10^{-4} \text{ M}$ ), (d) MB ( $3 \times 10^{-5} \text{ M}$ ), (e) R6G ( $4 \times 10^{-4} \text{ M}$ ), and  $\text{NaBH}_4$  ( $0.1 \text{ M}$ ,  $480 \mu\text{L}$ ).

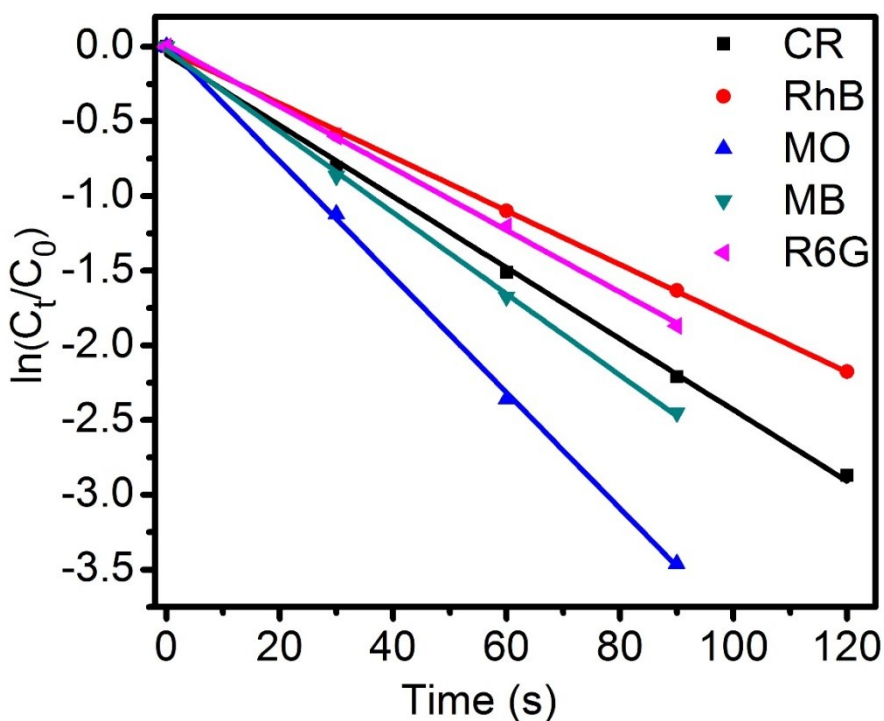


**Fig. S8** Calibration curves as a function of  $\ln(C_t/C_0)$  vs. reaction time for the reaction mixtures containing aqueous solutions of dyes (a) CR, (b) RhB, (c) MO, (d) MB, and (e) R6G in the presence of  $\text{NaBH}_4$  as a reducing agent and  $\text{MgAlCe-LDH@Au}$  ( $20 \mu\text{L}$ ,  $1 \text{ mg/mL}$ ) as a catalyst. Reaction conditions:  $\text{MgAlCe-LDH@Au}$  ( $20 \mu\text{L}$ ,  $1 \text{ mg/mL}$ ),  $2.5 \text{ mL}$  aqueous solutions of (a) CR ( $6 \times 10^{-5} \text{ M}$ ), (b) RhB ( $2 \times 10^{-6} \text{ M}$ ), (c) MO ( $1 \times 10^{-4} \text{ M}$ ), (d) MB ( $3 \times 10^{-5} \text{ M}$ ), (e) R6G ( $4 \times 10^{-4} \text{ M}$ ), and  $\text{NaBH}_4$  ( $0.1 \text{ M}$ ,  $480 \mu\text{L}$ ).

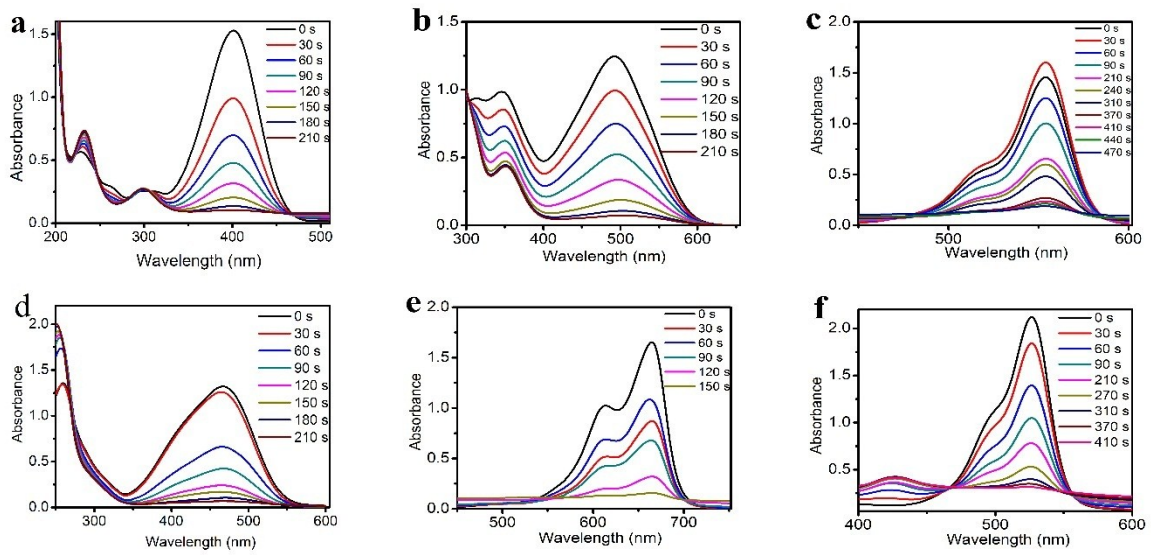


**Fig. S9** Time-dependent UV-vis spectra of the reaction mixtures containing (a) 4-NP, (b) CR, (c) RhB, (d) MO, (e) MB and (f) R6G aqueous solutions in the presence of NaBH<sub>4</sub> as a reducing agent and MgAl-LDH@Au as a catalyst. Reaction conditions: MgAl-LDH@Au (20  $\mu$ L, 1 mg/mL), 2.5 mL aqueous solutions of (a) 4-NP (10 mM) (b) CR ( $6 \times 10^{-5}$  M), (c) RhB ( $2 \times 10^{-6}$  M), (d) MO ( $1 \times 10^{-4}$  M), (e) MB ( $3 \times 10^{-5}$  M), (f) R6G ( $4 \times 10^{-4}$  M), and NaBH<sub>4</sub> (0.1 M, 200  $\mu$ L for 4-NP and 480  $\mu$ L for dyes).

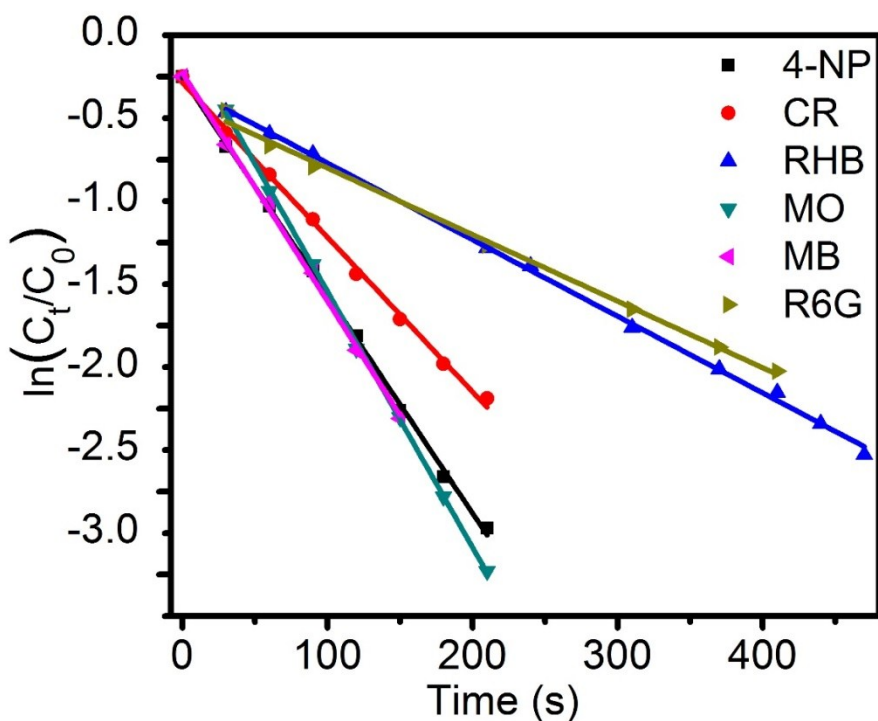


**Fig. S10** Calibration curves as a function of  $\ln(C_t/C_0)$  vs. reaction time for the reaction mixtures containing (a) 4-NP, (b) CR, (c) RhB, (d) MO, (e) MB and (f) R6G aqueous solutions in the presence of  $\text{NaBH}_4$  as a reducing agent and  $\text{MgAl-LDH@Au}$  as a catalyst. Reaction conditions:  $\text{MgAl-LDH@Au}$  ( $20 \mu\text{L}$ ,  $1 \text{ mg/mL}$ ),  $2.5 \text{ mL}$  aqueous solutions of (a) 4-NP ( $10\text{mM}$ ) (b) CR ( $6 \times 10^{-5} \text{ M}$ ), (c) RhB ( $2 \times 10^{-6} \text{ M}$ ), (d) MO ( $1 \times 10^{-4} \text{ M}$ ), (e) MB ( $3 \times 10^{-5} \text{ M}$ ), (f) R6G ( $4 \times 10^{-4} \text{ M}$ ), and  $\text{NaBH}_4$  ( $0.1 \text{ M}$ ,  $200 \mu\text{L}$  for 4-NP and  $480 \mu\text{L}$  for dyes).

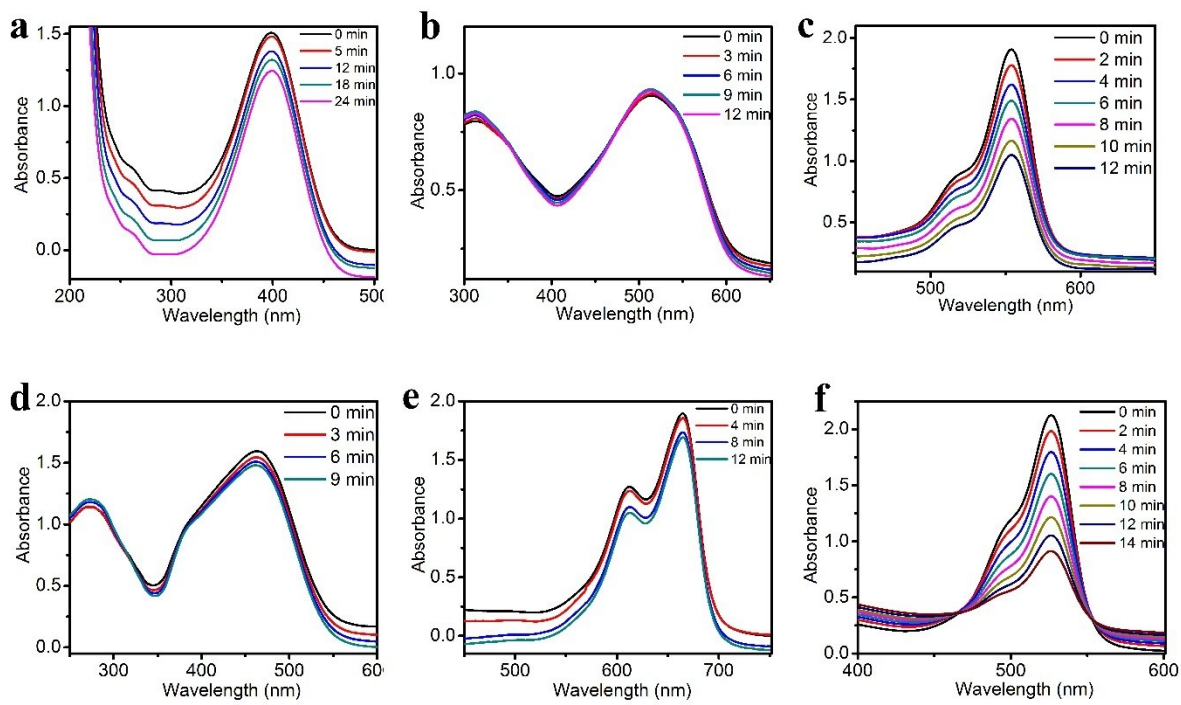


**Fig. S11** Time-dependent UV-vis spectra of the reaction mixtures containing (a) 4-NP, (b) CR, (c) RhB, (d) MO, (e) MB and (f) R6G aqueous solutions in the presence of  $\text{NaBH}_4$  as a reducing agent and MgAlCe-LDH as a catalyst. Reaction conditions: MgAlCe-LDH (20  $\mu\text{L}$ , 1 mg mL<sup>-1</sup>), 2.5 mL aqueous solutions of (a) 4-NP (10 mM), (b) CR ( $6 \times 10^{-5}$  M), (c) RhB ( $2 \times 10^{-6}$  M), (d) MO ( $1 \times 10^{-4}$  M), (e) MB ( $3 \times 10^{-5}$  M), (f) R6G ( $4 \times 10^{-4}$  M), and  $\text{NaBH}_4$  (0.1 M, 200  $\mu\text{L}$  for 4-NP and 480  $\mu\text{L}$  for dyes).

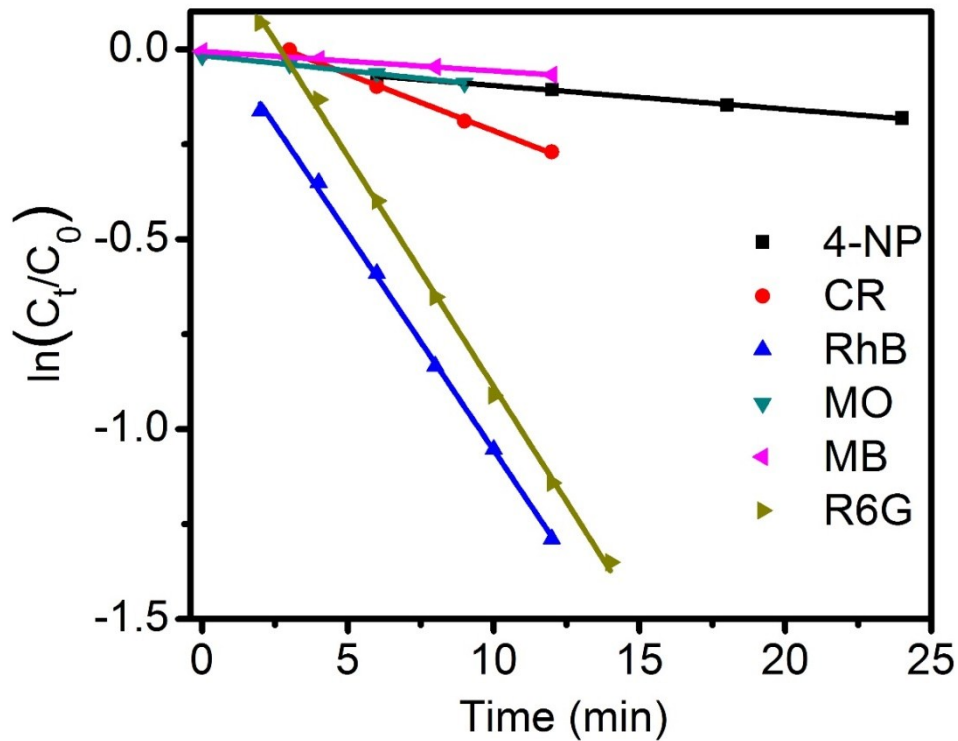


**Fig. S12** Calibration curves as a function of  $\ln(C_t/C_0)$  vs. reaction time for the reaction mixtures containing (a) 4-NP, (b) CR, (c) RhB, (d) MO, (e) MB, and (f) R6G aqueous solutions in the presence of  $\text{NaBH}_4$  as a reducing agent and MgAlCe-LDH as a catalyst. Reaction conditions: MgAlCe-LDH (20  $\mu\text{L}$ , 1 mg/mL), 2.5 mL aqueous solutions of (a) 4-NP (10 mM), (b) CR ( $6 \times 10^{-5}$  M), (c) RhB ( $2 \times 10^{-6}$  M), (d) MO ( $1 \times 10^{-4}$  M), (e) MB ( $3 \times 10^{-5}$  M), (f) R6G ( $4 \times 10^{-4}$  M), and  $\text{NaBH}_4$  (0.1 M, 200  $\mu\text{L}$  for 4-NP and 480  $\mu\text{L}$  for dyes).

**Table S1** Comparison of various catalytic systems for the reductive degradation of 4-NP.

Catalyst	Support	Reaction time (s)	$k_{app}$ (S <sup>-1</sup> )	TOF (h <sup>-1</sup> )	Reference
Au doped meso-porous Boehmite film	Boehmite film	1920	$1.7 \times 10^{-3}$	0.7	S1
PANI nanofiber/Au NPs	PANI	300	$11.7 \times 10^{-3}$	0	S2
AuNPs/SNTs nanocomposite	SNTs	280	$10.6 \times 10^{-3}$	46	S3
AuNPs@CSNFs	CSNFs	960	$5.9 \times 10^{-3}$	563	S4
Au@HSNs_C	SiO <sub>2</sub>	1800	$1.0 \times 10^{-3}$	14	S5
AuNPs@ZnO paper	Hydrogel ZnO	240	$2.4 \times 10^{-3}$	3	S6
Hollow capsule-stabilized Ag NPs	PAMAM	1800	$2.0 \times 10^{-3}$	196	S7
SiO <sub>2</sub> @Au/CeO <sub>2</sub>	SiO <sub>2</sub> @CeO <sub>2</sub>	300	$1.3 \times 10^{-2}$	240	S8
Micelle-supported Ag NPs	PNIPAP-b-P4VP	1950	$1.5 \times 10^{-3}$	16	S9
Au-DEND550-1	Au-DEND-PEG550	350	$9.4 \times 10^{-3}$	901	S10
Au(0)@TpPa-1	Au(0)@TpTa-1	780	$5.4 \times 10^{-3}$	9	S11
An NPs	Peptide	300	$1.3 \times 10^{-3}$	7	S12
$\alpha$ -CDS capped Au NPs	$\alpha$ -CD	600	$4.7 \times 10^{-3}$	34	S13
Au/graphene hydrogel	Graphene	720	$3.2 \times 10^{-3}$	12	S14
Au NPs	HPEI-IBAm	1140	-	120	S15
Au NPs/TWEEN/GO composites	TWEEN/GO	840	$4.2 \times 10^{-3}$	7	S16
Au-EGCG <sub>0.1</sub> -CF	EGCG-CF	1800	$2.4 \times 10^{-3}$	2	S17
DMF-stabilized Au NCs	DMF	4200	$3.0 \times 10^{-3}$	83	S18
Magnetically recoverable Au nanocatalyst	Chitosan	600	$1.2 \times 10^{-2}$	50	S19
Au-composite NPs	PDMAEMA-PS	750	$3.2 \times 10^{-3}$	1	S20
Pt1Au1-RGO	PDA/RGO	1800	$0.7 \times 10^{-3}$	14	S21
Pt3Au1-PDA/RGO	PDA/RGO	600	$9.6 \times 10^{-3}$	200	S21
Pt1Au1-PDA/RGO	PDA/RGO	600	$5.7 \times 10^{-3}$	118	S21
Au-PDA/RGO	PDA/RGO	600	$2.0 \times 10^{-3}$	42	S21
Au NPs	Solution B	120	$2.0 \times 10^{-2}$	$3.0 \times 10^3$	S22
Au NPs	Solution B	200	$9.0 \times 10^{-3}$	$9.0 \times 10^3$	S22
Au NPs	Solution B	1320	$1.0 \times 10^{-3}$	$5.5 \times 10^3$	S22
Fe <sub>3</sub> O <sub>4</sub> @CTS-Au NPs(A)	Fe <sub>3</sub> O <sub>4</sub>	1320	$8.6 \times 10^{-3}$	272	S23
Fe <sub>3</sub> O <sub>4</sub> @CTS-Au NPs(G)	Fe <sub>3</sub> O <sub>4</sub>	1320	$1.7 \times 10^{-2}$	296	S23
Fe <sub>3</sub> O <sub>4</sub> @C16@CTS-Au NPs(A)	Fe <sub>3</sub> O <sub>4</sub>	1320	$2.2 \times 10^{-2}$	413	S23
Fe <sub>3</sub> O <sub>4</sub> @C16@CTS-Au NPs(G)	Fe <sub>3</sub> O <sub>4</sub>	100	$3.1 \times 10^{-2}$	440	S23
<b>MgAl-LDH@Au</b>	<b>MgAl-LDH</b>	<b>210</b>	<b><math>1.3 \times 10^{-2}</math></b>	<b><math>3.4 \times 10^5</math></b>	<b>This work</b>
<b>MgAlCe-LDH@Au</b>	<b>MgAlCe-LDH</b>	<b>60</b>	<b><math>4.1 \times 10^{-2}</math></b>	<b><math>1.2 \times 10^6</math></b>	<b>This work</b>

**Table S2** Comparison of various catalytic systems for the reductive degradation of dyes: methylene blue (MB), methyl orange (MO), Congo red (CR), rhodamine B (RhB), and rhodamine 6G (R6G).

Catalyst	Support	Dye	Dye concentration	Reaction time (s)	$k_{app}$ (s <sup>-1</sup> )	TOF (h <sup>-1</sup> )	Reference
sFe <sub>3</sub> O <sub>4</sub> @C16@CT-S-Au NPs(G)	Fe <sub>3</sub> O <sub>4</sub>	MB	3.0 × 10 <sup>-5</sup> M	100	3.0 × 10 <sup>-8</sup>	114	S23
Au Nps/MCNSC	CNSs	MB	1 mM	720	3.3 × 10 <sup>-3</sup>	0	S24
Fe <sub>3</sub> O <sub>4</sub> @C@Au Nps	Fe <sub>3</sub> O <sub>4</sub> @C	MB	1.0×10 <sup>-7</sup> M	600	5.0 × 10 <sup>-3</sup>	0	S25
Au@TA-GH	Graphene	MB	0.63 μM	540	2.0 × 10 <sup>-3</sup>	26	S26
Au NPs	P.benghalensis	MB	10 mg mL <sup>-1</sup>	480	2.9 × 10 <sup>-3</sup>	-	S27
Au/KNbO <sub>3</sub>	KNbO <sub>3</sub>	MB	4.0 × 10 <sup>-5</sup> M	7200	2.0 × 10 <sup>-4</sup>	0.05	S28
Au NPs	S.acuminata fruit extract	MB	10 <sup>-4</sup> N	720	7.0 × 10 <sup>-4</sup>	0	S29
Au NPs	Kashayam	MB	9.4 × 10 <sup>-5</sup> M	300	5.5 × 10 <sup>-3</sup>	0	S30
Au NPs	Punica granatum	MB	1 mM	900	6.0 × 10 <sup>-3</sup>	0	S28
<b>MgAlCe-LDH@Au</b>	<b>MgAlCe-LDH</b>	<b>MB</b>	<b>3.0 × 10<sup>-5</sup> M</b>	<b>90</b>	<b>3 × 10<sup>-3</sup></b>	<b>2.2 × 10<sup>3</sup></b>	<b>This work</b>
Fe <sub>3</sub> O <sub>4</sub> @C16@CTS-Au NPs(G)	Fe <sub>3</sub> O <sub>4</sub>	MO	1.0 × 10 <sup>-4</sup> M	120	2.0 × 10 <sup>-2</sup>	304	S23
Au NPs	Punica granatum	MO	1 mM	900	3.0 × 10 <sup>-3</sup>	0	S28
Au NPs	S.acuminata fruit extract	MO	10 <sup>-4</sup> N	720	6.0 × 10 <sup>-4</sup>	0	S30
<b>MgAlCe-LDH@Au</b>	<b>MgAlCe-LDH</b>	<b>MO</b>	<b>1.0 × 10<sup>-4</sup> M</b>	<b>90</b>	<b>4.0 × 10<sup>-2</sup></b>	<b>8.0 × 10<sup>3</sup></b>	<b>This work</b>
Fe <sub>3</sub> O <sub>4</sub> @C16@CTS-Au NPs(G)	Fe <sub>3</sub> O <sub>4</sub>	CR	6.0 × 10 <sup>-5</sup> M	150	1.3 × 10 <sup>-2</sup>	149	S19
<b>MgAlCe-LDH@Au</b>	<b>MgAlCe-LDH</b>	<b>CR</b>	<b>6.0× 10<sup>-5</sup> M</b>	<b>120</b>	<b>2.4 × 10<sup>-2</sup></b>	<b>3.3 × 10<sup>3</sup></b>	<b>This work</b>
Fe <sub>3</sub> O <sub>4</sub> @C16@CTS-Au NPs(G)	Fe <sub>3</sub> O <sub>4</sub>	RhB	2.0× 10 <sup>-6</sup> M	140	1.6 × 10 <sup>-2</sup>	4.8	S19
<b>MgAlCe-LDH@Au</b>	<b>MgAlCe-LDH</b>	<b>RhB</b>	<b>2.0× 10<sup>-6</sup> M</b>	<b>120</b>	<b>2.0 × 10<sup>-2</sup></b>	<b>111</b>	<b>This work</b>
Fe <sub>3</sub> O <sub>4</sub> @C16@CTS-Au NPs(G)	Fe <sub>3</sub> O <sub>4</sub>	R6G	4.0 × 10 <sup>-4</sup> M	240	1.0 × 10 <sup>-2</sup>	626	S19
<b>MgAlCe-LDH@Au</b>	<b>MgAlCe-LDH</b>	<b>R6G</b>	<b>4.0× 10<sup>-4</sup> M</b>	<b>90</b>	<b>2.1 × 10<sup>-2</sup></b>	<b>2.9 × 10<sup>4</sup></b>	<b>This work</b>

## Supplementary References

- S1. D. Jana, A. Dandapat and G. De, *Langmuir*, 2010, 26, 12177-12184.
- S2. J. Han, L. Li and R. Guo, *Macromolecules*, 2010, 43, 10636-10644.
- S3. Z. Zhang, C. Shao, P. Zou, P. Zhang, M. Zhang, J. Mu, Z. Guo, X. Li, C. Wang and Y. Liu, *Chem. Commun.*, 2011, 47, 3906-3908.
- S4. H. Koga, E. Tokunaga, M. Hidaka, Y. Umemura, T. Saito, A. Isogai and T. Kitaoka, *Chem. Commun.*, 2010, 46, 8567-8569.
- S5. S.-H. Wu, C.-T. Tseng, Y.-S. Lin, C.-H. Lin, Y. Hung and C.-Y. Mou, *J. Mater. Chem.*, 2011, 21, 789-794.
- S6. H. Koga and T. Kitaoka, *Chem. Eng. J.*, 2011, 168, 420-425.
- S7. H. Wu, Z. Liu, X. Wang, B. Zhao, J. Zhang and C. Li, *J. Colloid. Interf. Sci.*, 2006, 302, 142-148.
- S8. B. Liu, S. Yu, Q. Wang, W. Hu, P. Jing, Y. Liu, W. Jia, Y. Liu, L. Liu and J. Zhang, *Chem. Commun.*, 2013, 49, 3757-3759.
- S9. Y. Wang, G. Wei, W. Zhang, X. Jiang, P. Zheng, L. Shi and A. Dong, *J. Mater. Chem. A.*, 2007, 266, 233-238.
- S10. N. Li, M. Echeverria, S. Moya, J. Ruiz and D. Astruc, *Inorg. Chem.*, 2014, 53, 6954-6961.
- S11. P. Pachfule, S. Kandambeth, D. D. Díaz and R. Banerjee, *Chem. Commun.*, 2014, 50, 3169-3172.
- S12. R. Bhandari and M. R. Knecht, *Catal. Sci. Technol.*, 2012, 2, 1360-1366.
- S13. T. Huang, F. Meng and L. Qi, *J. Phys. Chem. C.*, 2009, 113, 13636-13642.
- S14. J. Li, C.-y. Liu and Y. Liu, *J. Mater. Chem.*, 2012, 22, 8426-8430.
- S15. X.-Y. Liu, F. Cheng, Y. Liu, H.-J. Liu and Y. Chen, *J. Mater. Chem.*, 2010, 20, 360-368.
- S16. W. Lu, R. Ning, X. Qin, Y. Zhang, G. Chang, S. Liu, Y. Luo and X. Sun, *J. Hazard. Mater.*, 2011, 197, 320-326.
- S17. H. Wu, X. Huang, M. Gao, X. Liao and B. Shi, *Green. Chem.*, 2011, 13, 651-658.
- S18. H. Yamamoto, H. Yano, H. Kouchi, Y. Obora, R. Arakawa and H. Kawasaki, *Nanoscale*, 2012, 4, 4148-4154.
- S19. Y.-C. Chang and D.-H. Chen, *J. Hazard. Mater.*, 2009, 165, 664-669.
- S20. M. Zhang, L. Liu, C. Wu, G. Fu, H. Zhao and B. He, *Polymer*, 2007, 48, 1989-1997.
- S21. W. Ye, J. Yu, Y. Zhou, D. Gao, D. Wang, C. Wang and D. Xue *Appl. Catal. B Environ.*, 2016, 181, 371-378.
- S22. C. Deraedt, L. Salmon, S. Gatard, R. Ciganda, R. Hernandez, J. Ruiz and D. Astruc, *Chem. Commun.*, 2014, 50, 14194-14196.
- S23. J. Hu, Y.-I. Dong, Z. ur Rahman, Y.-h. Ma, C.-I. Ren and X.-g. Chen, *Chem. eng. J.*, 2014, 254, 514-523.
- S24. W. Zuo, G. Chen, F. Chen, S. Li and B. Wang, *RSC. Adv.*, 2016, 6, 28774-28780.
- S25. Z. Gan, A. Zhao, M. Zhang, W. Tao, H. Guo, Q. Gao, R. Mao and E. Liu, *Dalton Trans.*, 2013, 42, 8597-8605.
- S26. J. Luo, N. Zhang, J. Lai, R. Liu and X. Liu, *J. Hazard. Mater.*, 2015, 300, 615-623.
- S27. B. Paul, B. Bhuyan, D. D. Purkayastha, M. Dey and S. S. Dhar, *Mater. Lett.*, 2015, 148, 37-40.
- S28. L. Yan, T. Zhang, W. Lei, Q. Xu, X. Zhou, P. Xu, Y. Wang and G. Liu, *Catal. Today.*, 2014, 224, 140-146.
- S29. V. Suvith and D. Philip, *Spectrochim. Acta A Mol. Biomol. Spectrosc.*, 2014, 118, 526-532.
- S30. M. MeenaKumari and D. Philip, *Spectrochim. Acta A Mol. Biomol. Spectrosc.*, 2015, 135, 632-638.